We are IntechOpen, the world's leading publisher of Open Access books
Built by scientists, for scientists

6,900
Open access books available

185,000
International authors and editors

200M
Downloads

Our authors are among the

154
Countries delivered to

TOP 1%
most cited scientists

12.2%
Contributors from top 500 universities

CLARIVATE ANALYTICS
BOOK CITATION INDEX
INDEXED

WEB OF SCIENCE™

Selection of our books indexed in the Book Citation Index
in Web of Science™ Core Collection (BKCI)

Interested in publishing with us?
Contact book.department@intechopen.com

Numbers displayed above are based on latest data collected.
For more information visit www.intechopen.com

Thermoelectric Cooling: The Thomson Effect in Hybrid Two-Stage Thermoelectric Cooler Systems with Different Leg Geometric Shapes

Pablo Eduardo Ruiz-Ortega,
Miguel Angel Olivares-Robles and
Amado F. Garcia Ruiz

Abstract

This chapter aims to analyse the performance of hybrid two-stage thermoelectric cooler systems [two-stage thermoelectric cooling devices (TEC)], which are composed of different thermoelectric materials in each stage with different leg geometric shapes. If we consider a temperature gradient inside a two-stage TEC, then, besides Joule heat, also Thomson heat has to be taken into account. We discuss the out-of-equilibrium thermodynamics equations of a one-dimensional model to provide the performance expressions that govern the system. TEC system performance is analysed in function of the Thomson coefficients ratio of both stages. We describe a recent geometric optimization procedure that includes leg geometry parameters such as ratio of cross-sectional area and length of legs for each stage of the two-stage TEC.

Keywords: ideal equation (IE), Thomson effect, two-stage micro-cooler, Peltier effect

1. Introduction

Thermoelectric cooling devices are based on the Peltier effect to convert electrical energy into a temperature gradient. Thermoelectric effects, such as Seebeck effect, Peltier effect and Thomson effect, result from the interference of electrical current and heat flow in various semiconductor materials [1], and its interaction allows to use thermoelectric effects to generate electricity from a temperature differential; conversely, cooling phenomena occurs when a

voltage is applied across a thermoelectric material. Seebeck and Peltier effects depend on each other, and this dependence was demonstrated by W. Thomson who also showed the existence of a third thermoelectric effect, known as the Thomson effect. Thomson effect describes reversible heating or cooling, in a homogeneous semiconductor material, when there is both a flow of electric current and a temperature gradient [2, 3]. For thermoelectric cooling devices (TECs), a thermocouple consists of a p-type and n-type legs, with Seebeck coefficients (α) values positives and negatives respectively, joined by a conductor metal with low α value; in this chapter, we take this value as zero for calculations. Practical devices make use of modules that contain many thermocouples connected electrically in series and thermally in parallel [4]. TECs suffer from low efficiency, therefore, research on system geometry, for design and fabrication of thermoelectric cooling devices, is investigated in recent days [5, 6]. Coefficient of performance (*COP*) is the most important parameter for a thermoelectric cooling device, which is defined as the heat extracted from the source due an electrical energy applied [7]. Single-stage devices operate between a heat source and sink at a temperature gradient. However, multistage devices provide an alternative for extending the maximum temperature difference for a thermoelectric cooler. Therefore, two-stage coolers should be used to improve the cooling power, Q_c, and *COP*. In recent days, multistage thermoelectric cooling devices have been developed as many as six stages with bismuth telluride-based alloys. Recent works have investigated the ratio of the TE couple number between the stages and the effects of thermocouple physical size and have found that the cooling capacity is closely related to its geometric structure and operating conditions [8, 9]. In this chapter, a thermodynamics analysis and optimization procedure on performance of two-stage thermoelectric cooling devices based on the properties of established materials, system geometry and energy conversion, is analysed. Energy conversion issues in thermoelectric devices can be solved according to material properties: by increasing the magnitude of the differential Seebeck coefficient, by increasing the electrical conductivities of the two branches, and by reducing their thermal conductivities [10]. Several new theoretical and practical methods for the improvement of materials have been put forward and, at last, it seems that significant advances are being made, at least on a laboratory scale. In this work, we consider temperature-dependent properties material (TDPM) systems in calculations to determine the influence of the Thomson effect on performance [11, 12]. Many investigations have been conducted to improve the cooling capacity of two-stage TEC and found that cooling capacity is closely related to geometric structure and operating conditions of TECs. Our analysis to optimize cooling power of a thermoelectric micro-cooler (TEMC) includes a geometric optimization, that is, different cross-sectional areas for the p-type and n-type legs in both stages [13]. We find a novel procedure based on optimal material configurations, using two different semiconductors with different material properties, to improve the performance of a TEMC device with low-cost production.

This chapter is organized as follows: in Section 2, we give an overview of the thermoelectric effects. In Section 3, we apply thermodynamics theory to solve thermoelectric systems, and consequently, a description of the operation of a TEC device is presented. In Section 4, we proposed a two-stage TEC model taken into account Thomson effect for calculations to show its impact on *COP* and Qc. In Section 5, geometric parameters, cross-sectional area (A), and length (L) of a proposed two-stage TEMC system is analysed. For this purpose, constant

properties of materials (CPM) models and TDPM models are compared to show Thomson effect's impact on performance. We consider two cases: (a) the same materials in both stages (homogeneous system) and (b) different materials in each stage (hybrid system). We establish optimal configuration of materials that must be used in each stage. Finally, in Section 6, we present a discussion and concluding remarks.

2. Thermoelectric effects

Thermoelectricity results from the coupling of Ohm's law and Fourier's law. Thermoelectric effects in a system occur as the result of the mutual interference of two irreversible processes occurring simultaneously in the system, namely heat transport and charge carrier transport [14]. To define Seebeck and Peltier coefficients, we refer to the basic thermocouple shown in **Figure 1**, which consists of a closed circuit of two different semiconductors. For a thermocouple composed of two different materials a and b, the voltage is given by:

$$V_{ab} = \int_{1}^{2} (\alpha_b - \alpha_a) dT \tag{1}$$

where the parameters α_a and α_b are the Seebeck coefficients for semiconductor materials a and b.
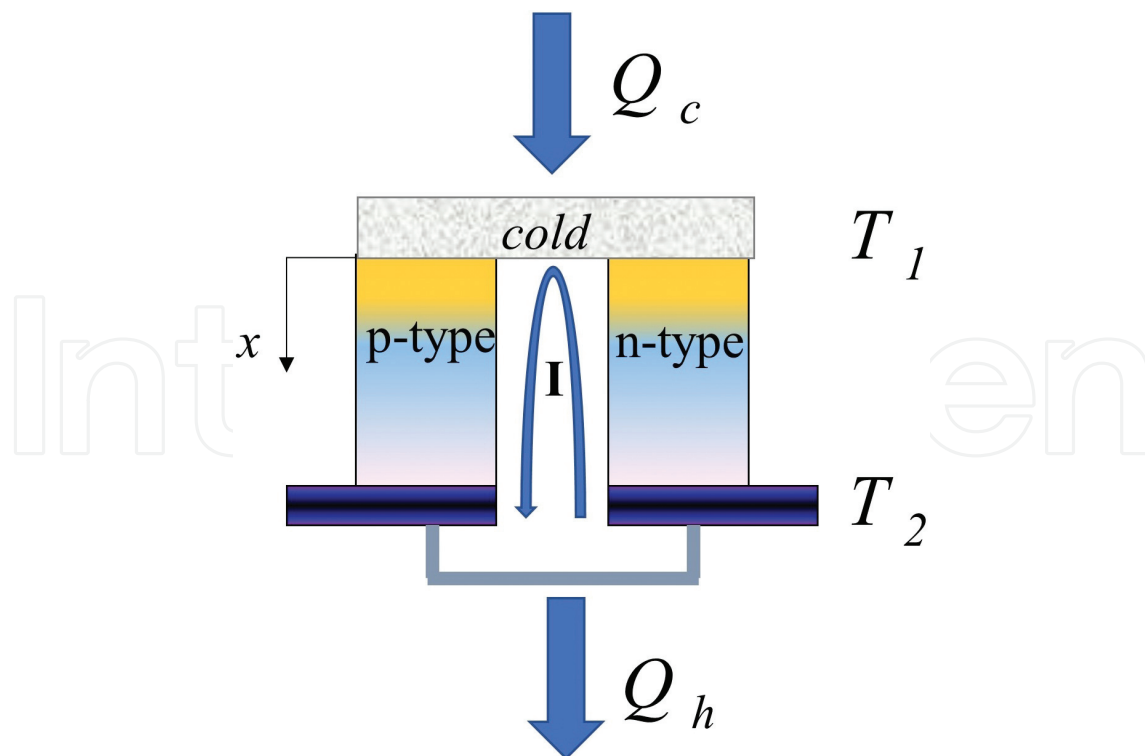
Figure 1. Single thermocouple model for a TEC system.

The differential Seebeck coefficient, under open-circuit conditions, is defined as the ratio of the voltage, V, to the temperature gradient, ΔT

$$\alpha_{ab} = \frac{V}{\Delta T} \tag{2}$$

Electrons move through the n-type element towards the positive pole, attraction effect, while the negative pole of the voltage source repels them. Likewise, in the p-type semiconductor, the holes move to the negative potential of the voltage source, while positive potential acts as repel of the holes and they move in the contrary direction to the flow of electrons. As a result, in p-type semiconductors, α is positive and in n-type semiconductors, α is negative [15]. Peltier coefficient is equal to the rate of heating or cooling, Q, ratio at each junction to the electric current, I. The rate of heat exchange at the junction is

$$Q = \pi_{ab}I \tag{3}$$

Peltier coefficient is regarded as positive if the junction at which the current enters is heated and the junction at which it leaves is cooled. When there is both an electric current and a temperature gradient, the gradient of heat flux in the system is given by

$$\frac{dQ}{dx} = \tau I \frac{dT}{dx} \tag{4}$$

where x is a spatial coordinate and T the temperature. Thomson coefficient, known as the effect of liberate or absorb heat due to an electric current flux through a semiconductor material in which exist a temperature gradient, is given by the Kelvin relation as follows

$$\tau_a - \tau_b = T\frac{d\alpha_{ab}}{dT} \tag{5}$$

When Seebeck coefficient is considered independent of temperature, Thomson coefficient will not be taken into account in calculations, τ is zero.

2.1. Thomson relations

Seebeck effect is a combination of the Peltier and Thomson effects [16]. The relationship between temperature, Peltier, and Seebeck coefficient is given by the next Thomson relation

$$\pi_{ab} = \alpha_{ab}T \tag{6}$$

These last effects have a relation to the Thomson coefficient, τ, given by

$$\tau = T\frac{d\alpha}{dT} \tag{7}$$

To develop an irreversible thermodynamics theory, Thomson's theory of thermoelectricity plays a remarkable role, because this theorem is the first attempt to develop such theory.

3. Thermoelectric refrigeration in nonequilibrium thermodynamics framework

Theory of thermoelectric cooling is analysed according to out-of-equilibrium thermodynamics. Under isotropic conditions, when an electrical current density flows through the semiconductor material with a temperature gradient and steady-state condition, the heat transport and charge transport relations, consistent with the Onsager theory [17], are

$$j_{el} = \sigma E - \sigma \alpha \nabla T \tag{8}$$

and

$$j_q = \alpha T j_{el} - \kappa \nabla T \tag{9}$$

where, α is the Seebeck coefficient, T is the temperature, κ is the thermal conductivity, E is the electric field, j_{el} is the electric current density, j_q is the heat flux and σ is the electric conductivity. Equation (9) is the essential equation for thermoelectric phenomena. The governing equations are

$$\nabla \cdot j_{el} = 0 \quad \text{and} \quad \nabla \cdot j_q = j_{el} \cdot E \tag{10}$$

For one-dimensional model, from Equations (8) and (9), we get for the heat flux

$$\vec{\nabla} \cdot \left(\kappa \, \vec{\nabla} \, T \right) + j^2 \rho - T \frac{d\alpha}{dT} \vec{J} \cdot \vec{\nabla} \, T = 0 \tag{11}$$

where ρ is the electrical resistivity ($\rho = 1/\sigma$) and J is the electric current density. In Equation (11), the first term describes the thermal conduction due to the temperature gradient. According to Fourier's law, the second term is the joule heating and the third term is the Thomson heat, both depending on the electric current density [18]. Now, from Equation (11), the equation that governs the system for one-dimensional steady state is given by:

$$\kappa(T) \frac{\partial^2 T}{\partial x^2} + \frac{d\kappa}{dT} \left(\frac{\partial T}{\partial x} \right)^2 - jT \frac{d\alpha}{dT} \frac{\partial T}{\partial x} = -\frac{j^2}{\sigma(T)} \tag{12}$$

3.1. Cooling power

Thermoelectric coolers make use of the Peltier effect which origin resides in the transport of heat by an electric current. For this analysis, we assume that thermal conductivity, electrical resistivity, and Seebeck coefficient are all independent of temperature, that is, CPM model [19], and the metal that connects the p-type with the n-type leg has a low α value, therefore it is considered as zero. We assume that there is zero thermal resistance between the ends of the branches and the heat source and sink. Thus, only electrical resistance is considered for the thermocouple legs, thereby, the thermocouple legs are the only paths to transfer heat between the source and sink, conduction via the ambient, convection, and radiation are ignored. These

considerations have been addressed in previous studies showing that the *COP* does not depend on the semiconductors length when the electrical and thermal contact resistances are not considered in calculations [20]. To determine the coefficient of performance (*COP*), which is defined as the ratio of the heat extracted from the source to the expenditure of electrical energy, a thermocouple model shown in **Figure 1** is used. Thus, for the p-type and n-type legs, the heat transported from the source to the sink is

$$Q_p = \alpha_p IT - K_p A_p \frac{dT}{dx}; \qquad Q_n = -\alpha_n IT - K_n A_n \frac{dT}{dx} \tag{13}$$

where A is the cross-sectional area, K is the thermal conductivity, and dT/dx is the temperature gradient. Heat is removed from the source at the rate

$$Q_c = \left(Q_p + Q_n\right)|_{x=0} \tag{14}$$

The rate of generation of heat per unit length from the Joule effect is $I^2\rho/A$. This heat generation implies that there is a non-constant thermal gradient

$$-\kappa_p A_p \frac{d^2T}{dx^2} = \frac{I^2\rho_p}{A_p}; \qquad -\kappa_n A_n \frac{d^2T}{dx^2} = \frac{I^2\rho_n}{A_n} \tag{15}$$

Using next boundary conditions: $T = T_1$ at $x = 0$ and $T = T_2$ at $x = L$, we get

$$\kappa_{n,p} A_{n,p} \frac{dT}{dx} = -\frac{I^2\rho_{n,p}\left(x - L_{n,p}/2\right)}{A_{n,p}} + \frac{\kappa_{n,p} A_{n,p}(T_2 - T_1)}{L_{n,p}} \tag{16}$$

where the subscripts n and p are for the n-type and p-type elements, respectively. From Equation (10), we find for the cooling power at the cold side $x = 0$

$$Q_c = \left(\alpha_p - \alpha_n\right)IT_1 - K\Delta T - \frac{1}{2}I^2R \tag{17}$$

where $\Delta T = T_2 - T_1$. The thermal conductance of the two legs in parallel is

$$K = \frac{\kappa_p A_p}{L_p} + \frac{\kappa_n A_n}{L_n} \tag{18}$$

and the electrical resistance of the two legs in series is

$$R = \frac{L_p\rho_p}{A_p} + \frac{L_n\rho_n}{A_n} \tag{19}$$

3.2. Coefficient of performance

The total power consumption in the TEC system is

$$W = (\alpha_p - \alpha_n)I\Delta T + I^2 R \tag{20}$$

then, the coefficient of performance in a TEC system is defined as [21]

$$COP = \frac{Q_c}{W} \tag{21}$$

4. Thomson effect impact on performance of a two-stage TEC

4.1. One-dimensional formulation of a physical two-stage TEC

To determine analytical expressions of cooling power and coefficient of performance in a two-stage TE system, we establish one-dimensional representation model, as shown in **Figure 2**. When a voltage is applied across the device, as a result, an electric current, I, flows from the positive to the negative terminal [22, 23].

$T_1 = T_c$, Q_{c1}, and Q_{h1} are, respectively, cold junction side temperature, amount of heat that can be absorb and amount of heat rejected from stage 1 to 2 of TEC. $T_2 = T_h$, Q_{h2} and Q_{c2} are, respectively, hot junction temperature, amount of heat rejected to the heat source and amount of heat absorbed from stage 1. It should be noted that Q_m is the heat flow from stage 1 to stage 2, that is, $Q_m = Q_{h1} = Q_{c2}$, and T_m is the average temperature in the system. For calculations, we use TDPM model [24] in order to show Thomson effect's role in the system. Arranging pairs of elements in this way allows the heat to be pumped in the same direction.

4.2. TEC electrically connected in series

Considering model from **Figure 2**, we get temperature distributions for p-type and n-type semiconductor legs in each stage. T_{11} and T_{12} are, respectively, the temperatures at the cold side junction for p-type and n-type legs in stage 1. T_{21} and T_{22} are, respectively, the temperatures at the hot side junction for p-type and n-type legs in stage 2 [25]. Solving with next boundary conditions: $T_{11}(0) = T_{12}(0) = T_1$ and $T_{11}(L_{11}) = T_{12}(L_{12}) = T_m$, we have for the first stage

$$T_{1(1,2)} = T_{(1,m)} \mp A_{1(1,2)}x + \frac{\Delta T \pm A_{1(1,2)}L_{1(1,2)}}{1 - e^{\mp \omega_{1(1,2)}L_{1(1,2)}}}(1 - e^{\mp \omega_{1(1,2)}x}), \, 0 \leq x \leq L_{1(1,2)} \tag{22}$$

and for the second stage, with $T_{21}(L_{11}) = T_{22}(L_{12}) = T_m$ and $T_{21}(L_{21}) = T_{22}(L_{22}) = T_h$

$$T_{2(1,2)} = T_{(m,2)} \mp A_{2(1,2)}x + \frac{\Delta T \pm A_{2(1,2)}L_{2(1,2)}}{1 - e^{\mp \omega_{2(1,2)}L_{2(1,2)}}}(1 - e^{\mp \omega_{2(1,2)}x}), \, L_{1(1,2)} \leq x \leq L_{2(1,2)} \tag{23}$$

where $\omega_{ij} = \frac{\tau_{ij}I}{K_{ij}L_{ij}}$, $A_{ij} = \frac{R_{ij}I}{\tau_{ij}L_{ij}}$, $K_{ij} = \frac{\kappa_{ij}S_{ij}}{L_{ij}}$, $R_{ij} = \frac{L_{ij}}{\sigma_{ij}S_{ij}}$ for $i = 1, 2$ and $j = 1, 2$ when $i \geq j$. The subscripts 1 and 2 describe cold temperature and hot temperature in the junctions. According to the theory of non-equilibrium thermodynamics, for the TEMC, we have for the first stage [26],
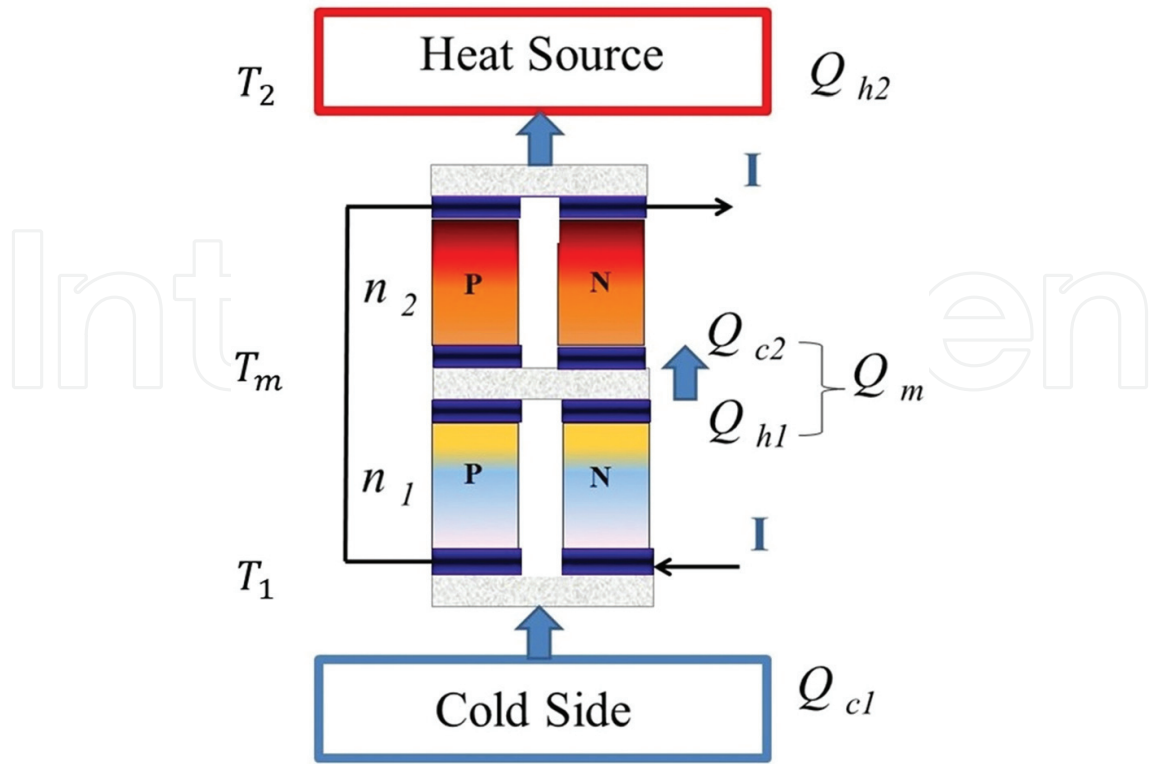
Figure 2. Two-stage thermoelectric cooler (TEC), electrically connected in series.

$$Q_{c1} = \alpha_1^c T_c I - K_1^*(T_m - T_c) - (R_1^* + R_1)I^2 \tag{24}$$

$$Q_{h1} = \alpha_1^m T_m I - K_1^*(T_m - T_c) - \tau_1(T_m - T_c) - R_1^* I^2 \tag{25}$$

$$Q_{c2} = \alpha_2^m T_m I - K_2^*(T_h - T_m) - (R_2^* + R_2)I^2 \tag{26}$$

$$Q_{h2} = \alpha_2^h T_h I - K_2^*(T_h - T_m) - \tau_2(T_h - T_m) - R_2^* I^2 \tag{27}$$

with $\alpha_1^k = \alpha_{12}^k - \alpha_{11}^k$, for $k = c, m$ and $\alpha_2^l = \alpha_{22}^l - \alpha_{21}^l$, for $l = m, h$; $R_j = R_{j1} + R_{j2}$; $\tau_j = \tau_{j2} - \tau_{j1}$ and $R_j^* = \left[R_{j1}^* + R_{j2}^* - (R_{j1} + R_{j2}) \right]$ for $j = 1, 2$. A general solution for the heat fluxes in two-stage system is found in [27] where Thomson effect is studied. The system's coefficient of performance, COP, is determined by Q_c and Q_h as follows

$$COP = \frac{\alpha_2^h T_h I - K_2^*(T_h - T_m) - \tau_2(T_h - T_m) - R_2^* I^2}{K_1^*(T_m - T_c) + (T_h - T_m)(-\tau_2 I - K_2^*) + (\alpha_2^h T_h - \alpha_1^c T_c)I + (R_1^* + R_1 - R_2^*)I^2} \tag{28}$$

Performance depends on Thomson coefficients values of both the first stage and the second stage. In our results, we show the role of the ratio values of the Thomson coefficients, $\tau_r = \tau_1/\tau_2$ between stages, on performance. Now solving for T_m, knowing that $Q_m = Q_{h1} = Q_{c2}$, from Equations (25) and (26)

$$T_m = \frac{I^2\left(R_1^* - R_2^* - R_2\right) - T_c\left(K_1^* + \tau_1 I\right) - K_2^* T_h}{I\left(\alpha_1^m - \alpha_2^m - \tau_1\right) - \left(K_1^* + K_2^*\right)} \tag{29}$$

where $K_j^* = K_{j1}^* + K_{j2}^*$, $K_{j1}^* = \frac{\tau_{j1} I}{1 - e^{-\omega_{j1} L_{j1}}}$, $K_{j2}^* = \frac{\tau_{j2} I}{e^{\omega_{j2} L_{j2}} - 1}$, $R_{j1}^* = R_{j1}\left(\frac{1}{1 - e^{-\omega_{j1} L_{j1}}} - \frac{1}{\omega_{j1} L_{j1}}\right)$ and $R_{j2}^* = R_{j2}\left(\frac{1}{\omega_{j2} L_{j2}} - \frac{1}{e^{\omega_{j2} L_{j2}} - 1}\right)$ for $j = 1, 2$. Once again we must notice the relationship that exists between both stages according to average temperature T_m, which also depends on the Thomson effect.

4.2.1. Influence of Thomson effect on performance (COP) and cooling power (Q_c)

Two different materials were used for calculations, thermoelectric properties are shown in **Table 1**, where only Seebeck coefficient is consider that depends on temperature.

With $\alpha_1 = \left[2 \times 10^{-4} + 2 \times 10^{-2}\ (1/T_m - 1/T)\right]$ for material $Bi_2 Te_3$ and $\alpha_2 = [-62675 + 1610\ T - 2.3\ T^2] \times 10^{-6}$ and for material $(Bi_{0.5}Sb_{0.5})Te_3$ [25].

Figure 3 shows the *COP* and the cooling power Q_c, in function of τ_r, at different electric current values $Bi_2 Te_3$ and $(Bi_{0.5}Sb_{0.5})Te_3$ [28]. It is clear that *COP* behaviour is influenced directly by the Thomson effect ratio of both stages. *COP* values increase when there is an increase in the ratio τ_r for lower values of the electric current I. We must notice that for lower values of $\tau_r < 1$, *COP* values are very closely one with another, with a maximum difference of 17% as compared an

Property	Bi_2Te_3	$\left(Bi_{0.5}\,Sb_{0.5}\right)_2 Te_3$	Unit
$\bar{\alpha}_{1,2}$	197.7×10^{-6} (at 288K)	210.3×10^{-6} (at 288K)	V/K
$\kappa_{1,2}$	1.6	1.35	W/mK
$\rho_{1,2}$	$0.7\,x10^{-5}$	$1.5385\,x10^{-5}$	Ωm

Table 1. Properties of thermoelectric (TE) elements.
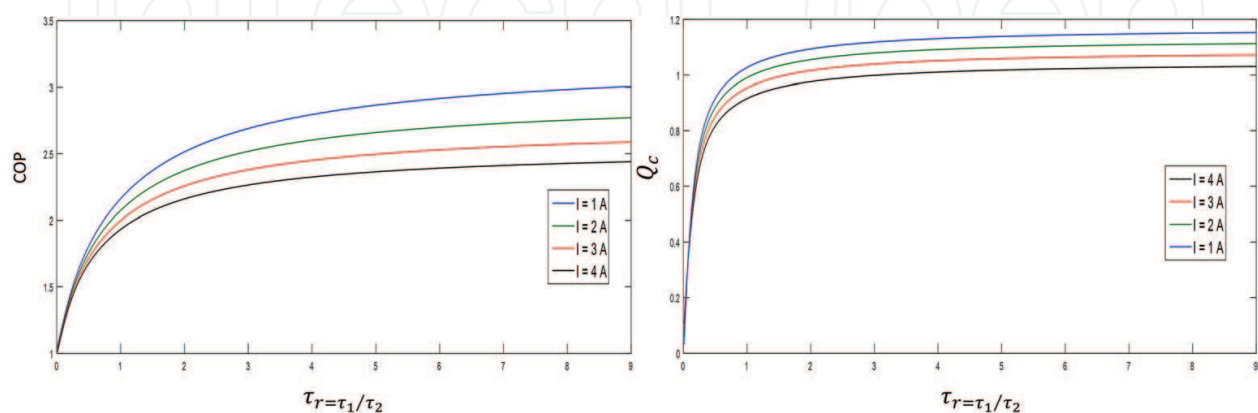
Figure 3. *COP* and Q_c in function of the ratio $\tau_r = \frac{\tau_1}{\tau_2}$, for different electric current values I.

electric current value of 1 A with an electric current of 4 A, when $\tau_r = 1$. Moreover, it is observed that from values of $\tau_r > 2$ COP values increase for all the different electric current values.

Similar behaviour, to what happens with the performance COP, happens for the cooling power Q_c, where maximum values are obtained for higher values of τ_r, as shown in **Figure 3**. In this case, Q_c value for an electric current value of 1 A is 11 % higher compared with electric current values of 4 A, when $\tau_r = 1$.
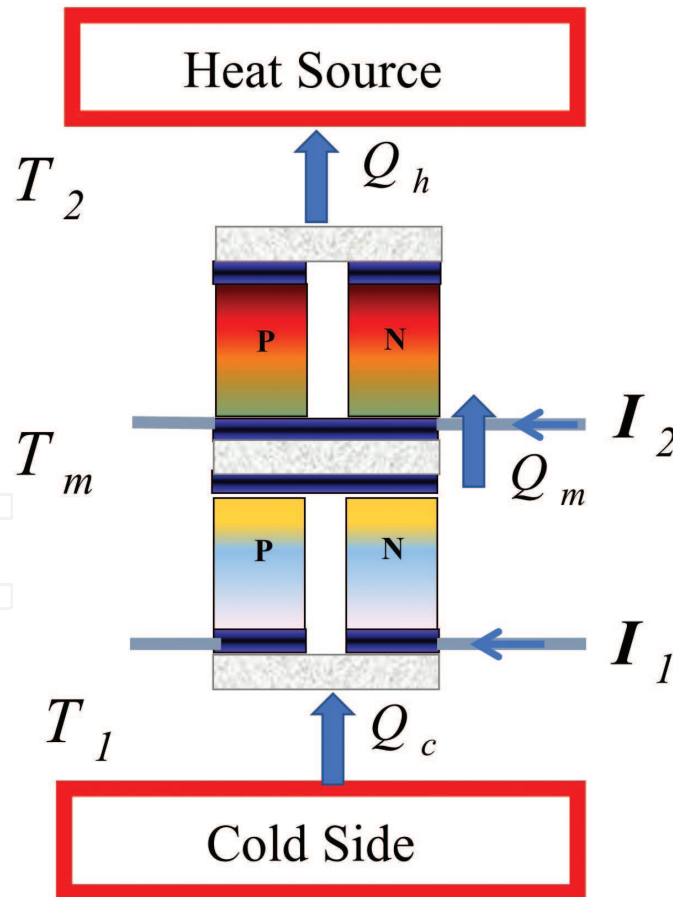
4.3. TECs electrically connected in parallel

Now, we analyse the case in which different electric currents flow in each stage of the system (**Figure 4**). The ratio of electric currents between each stage is given by

$$I_r = \frac{I_1}{I_2} \tag{30}$$

$$Q_c = \alpha_1^c T_c I_1 - K_1^*(T_m - T_c) - (R_1^* + R_1)I_1^2 \tag{31}$$

$$Q_{m1} = \alpha_1^m T_m I_1 - K_1^*(T_m - T_c) - \tau_1(T_m - T_c) - R_1^* I_1^2 \tag{32}$$

Figure 4. Two-stage thermoelectric cooler (TEC), electrically connected in parallel. Now, in the same way as in the previous section, we solve for the heat fluxes in the system.

$$Q_{m2} = \alpha_2^m T_m I_2 - K_2^*(T_h - T_m) - (R_2^* + R_2)I_2^2 \tag{33}$$

$$Q_h = \alpha_2^h T_h I_2 - K_2^*(T_h - T_m) - \tau_2(T_h - T_m) - R_2^* I_2^2 \tag{34}$$

where I_1 is the electric current flow in stage 1 and I_2 is the electric current flow in stage 2.

According to the continuity of the heat flow between both stages, $Q_{m1} = Q_{m2}$, from Equations (32) and (33), we solve for the average temperature, T_m

$$T_m = \frac{R_1^* I_1^2 - \tau_1 T_c I_1 - K_1^* T_c - K_2^* T_h - (R_2^* + R_2)I_2^2}{I_1(\alpha_1^m - \tau_1) - (K_1^* + K_2^*) - \alpha_2^m I_2} \tag{35}$$

The system's coefficient of performance, COP, is given by

$$COP = \frac{\alpha_2^h T_h I_2 - K_2^*(T_h - T_m) - \tau_2(T_h - T_m) - R_2^* I_2^2}{\left(\alpha_2^h T_h I_2 - K_2^*(T_h - T_m) - \tau_2(T_h - T_m) - R_2^* I_2^2\right) - \alpha_1^c T_c I_1 - K_1^*(T_m - T_c) - (R_1^* + R_1)I_1^2} \tag{36}$$

In the previous section, it is shown that COP increases for higher values of Thomson coefficient ratio between both stages. The behaviour of the COP for the case where two different electric currents flow in the system, shown in **Figure 5**, is now analysed. Three different values of
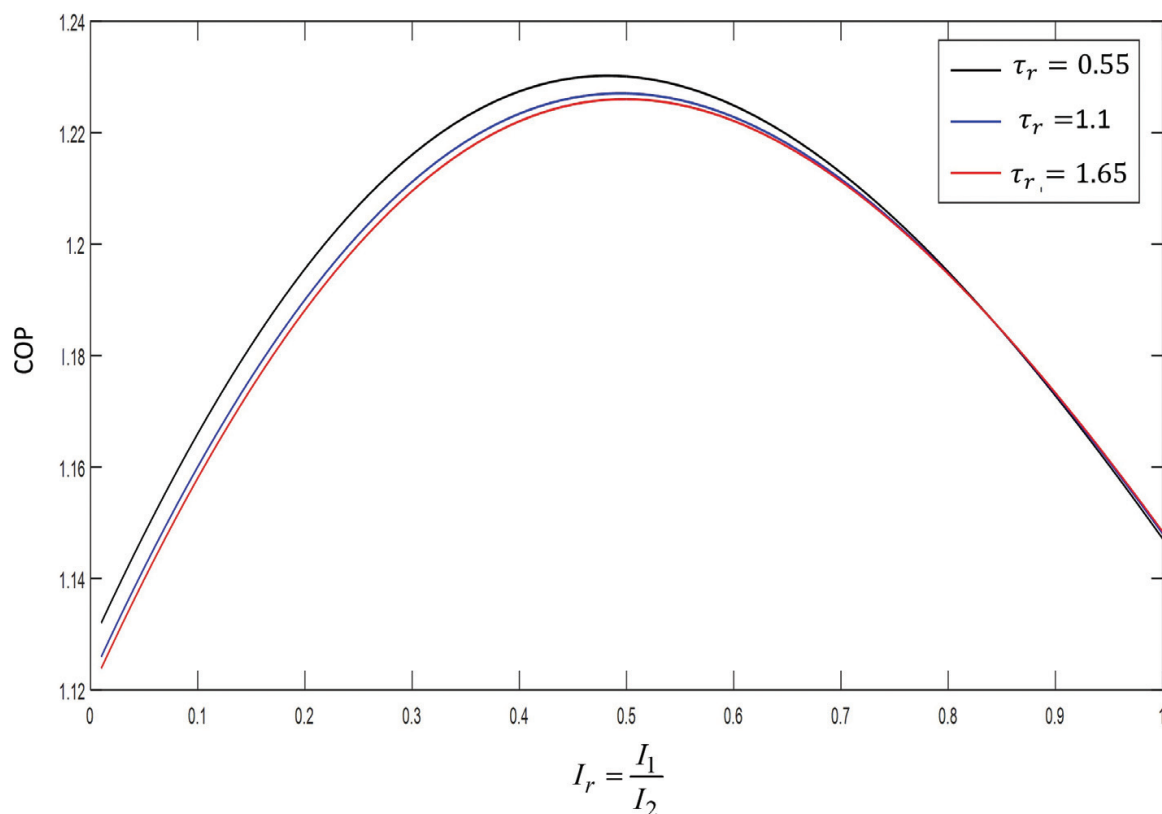
Figure 5. COP in function of the ratio $I_r = \frac{I_1}{I_2}$, for different τ_r values.

τ_r	COP_{max}	I_r
0.55	1.23	0.49
1.1	1.227	0.51
1.65	1.228	0.513

Table 2. Maximum values of *COP*.

Thomson coefficients, τ_r, are considered. **Table 2** shows maximum values, from **Figure 5**, for *COP* in function of the electric current ratio between both stages, I_r. Maximum *COP* value is obtained for higher values of the ratio τ_r, that is, a higher value of the electric current $I_2 > I_1$ is desirable to be able to achieve better *COP*.

5. Dimensionless equations of a two-stage thermoelectric micro-cooler

Once it has been investigated the role of the Thomson heat on TEC performance, now a procedure to improve the performance of the micro-cooler based on optimum geometric parameters, cross-sectional area (A) and length (L), of the semiconductor elements is proposed. To optimal design of a TEMC, theoretical basis on optimal geometric parameters (of the p-type and n-type semiconductor legs) is required. Next analysis of a TEMC includes these optimization parameters. The configuration of a two-stage TE system considered in this work is shown in **Figure 2**. Each stage is made of different thermoelectric semiconductor materials. In order to make Equation (12) dimensionless using the boundary conditions $T(0) = T_1$ and $T(L) = T_2$, in accordance with **Figure 2**, we define the dimensionless temperature, θ, and the ξ parameter as,

$$\theta = \frac{T - T_1}{T_2 - T_1} \text{ and } \xi = \frac{x}{L} \tag{37}$$

Dimensionless differential equation corresponding to Equation (12) is given by:

$$\frac{d^2\theta}{d\xi^2} - \beta\big((\theta - 1)\phi + 1\big)\frac{d\theta}{d\xi} + \gamma = 0 \tag{38}$$

where

$$\beta = \frac{IT_2 \frac{d\alpha}{dT}\Delta T}{A\kappa\frac{\Delta T}{L}} \tag{39}$$

that is, β is the relation between Thomson heat with thermal conduction. From Equation (38), if $\beta = 0$, we get the ideal equation (IE) when Thomson effect not considered. Dimensionless parameter, γ, is the relation between Joule heating to the thermal conduction, and the parameter ϕ, which is the ratio of temperature difference to the high junction temperature, defined as:

$$\gamma = \frac{I^2 R}{A\kappa \frac{\Delta T}{L}} \quad \text{and} \quad \phi = \frac{\Delta T}{T_2} \tag{40}$$

5.1. Cooling power: the ideal equation and Thomson effect (τ)

If we consider Seebeck coefficient independent of temperature, Thomson coefficient is negligible ($\beta = 0$), we can obtain the exact result for the cooling power at the cold junction from Equation (14), which is called the ideal equation (IE) for cooling power

$$\dot{Q}_c^{IE} = \overline{\alpha} T_1 I - \frac{1}{2} I^2 R - \frac{Ak}{L}(T_2 - T_1) \tag{41}$$

The resulting equation considering the Thomson effect is given by:

$$\dot{Q}_c^{\beta} = \overline{\alpha} T_1 I - \frac{1}{2} I^2 R - \frac{Ak}{L}(T_2 - T_1) + \beta \frac{Ak}{L}(T_2 - T_1) \tag{42}$$

5.2. Geometric parameter between stages: area-length ratio (W = $w1/w2$)

Figure 6 shows a simple thermocouple with length, L and cross-sectional area, A. Previous studies proved that an improvement on performance of TECs can be achieved by optimizing
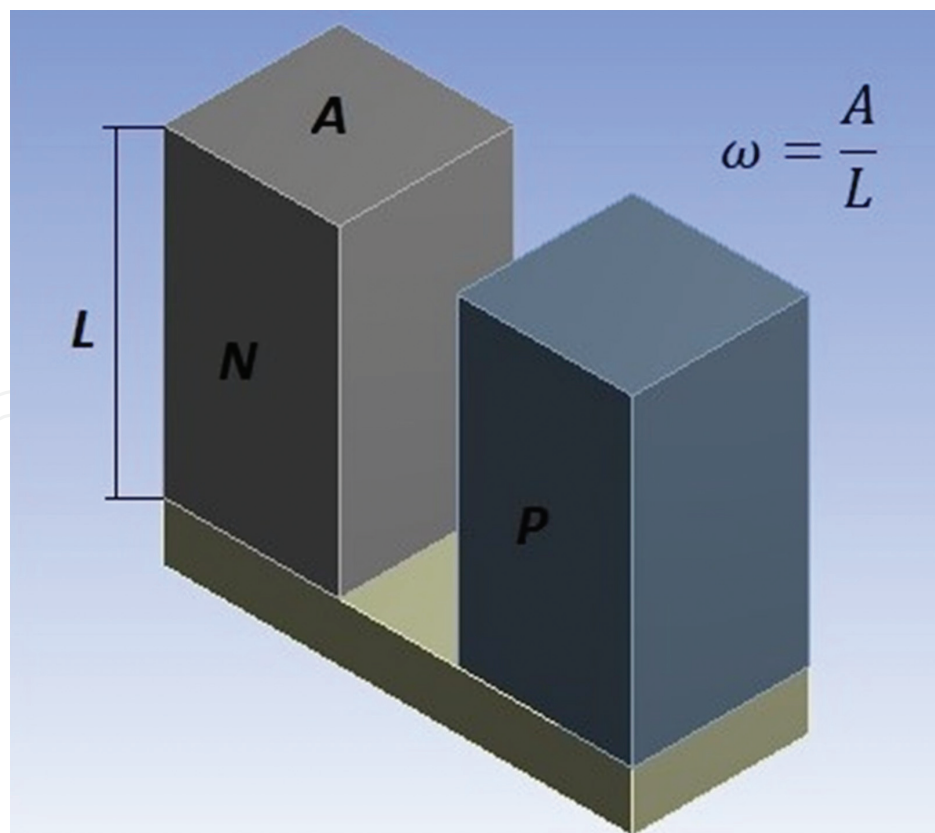
Figure 6. Schematic diagram of a thermocouple.

geometric size of the semiconductor legs [29, 30]. A geometric parameter, ω, is defined as the area-length ratio of the legs in the thermocouple in each stage of the TEMC

$$\omega_1 = \frac{A_1}{L_1} \quad \text{and} \quad \omega_2 = \frac{A_2}{L_2} \tag{43}$$

for the first and second stage, respectively.

We define the geometric parameter, W, which allows us to determine the optimal geometric parameters of the stages, which is expressed as,

$$W = \frac{\omega_1}{\omega_2} \tag{44}$$

In terms of the geometric parameters, ω_1 and ω_2, we get:

$$R = R_p + R_n = \frac{L_p}{\sigma_p A_p} + \frac{L_n}{\sigma_n A_n} = \frac{1}{\sigma_p \omega_1} + \frac{1}{\sigma_n \omega_2} \tag{45}$$

$$K = K_p + K_n = \frac{A_p k_p}{A_p} + \frac{A_n k_n}{A_n} = \omega_1 k_p + \omega_2 k_n \tag{46}$$

We have for the cooling power, in terms of the geometric parameters, ω_1 and ω_2

$$\dot{Q}_c^{IE} = \alpha(T_{avg}) T_1 I - \frac{1}{2} I^2 \left(\frac{1}{\sigma_p \omega_1} + \frac{1}{\sigma_n \omega_2} \right) - (\omega_1 k_p + \omega_2 k_n)(T_2 - T_1) \tag{47}$$

For ideal equation, $\dot{Q}_c^{IE}$, and Thomson effect, $\dot{Q}_c^{\beta}$, we have

$$\dot{Q}_c^{\beta} = \alpha(T_{avg}) T_1 I - \frac{1}{2} I^2 \left(\frac{1}{\sigma_p \omega_1} + \frac{1}{\sigma_n \omega_2} \right) - (\omega_1 k_p + \omega_2 k_n)(T_2 - T_1) + \beta(\omega_1 k_p + \omega_2 k_n)(T_2 - T_1) \tag{48}$$

Finally, we introduce the ratio, M, of the number of thermocouples in the first stage, n_1, to the number of thermocouples in second stage, n_2

$$M = \frac{n_1}{n_2} \tag{49}$$

The total number of thermocouples, N, for both stages is given by,

$$N = n_1 + n_2 \tag{50}$$

5.3. Material properties considerations: CPM and TDPM models

The two different semiconductor materials and their properties are given in **Table 3**: Material M_1, which is obtained from commercial module of laird $CP10 - 127 - 05$ and its properties

Property	Material 1, $CP10-127-05$	Material 2, $(Bi_{0.5}Sb_{0.5})_2Te_3$	Unit
$\bar{\alpha}_{1,2}$	198.34×10^{-6} (at 288 K)	210.3×10^{-6} (at 288 K)	V/K
$\kappa_{1,2}$	1.6	1.35	W/mK
$\rho_{1,2}$	1.01×10^{-5}	1.5385×10^{-5}	Ωm

Table 3. Properties of thermoelectric (TE) elements used in the TEMC device.

were provided by the manufacturer [21], and material M_2, $(Bi_{0.5}Sb_{0.5})_2Te_3$ [17], $T_{avg} = (T_1 + T_2)/2$, where $\bar{\alpha} = \alpha(T_{avg})$ and Seebeck coefficients are dependent on temperature while the electrical resistivity and the thermal conductivity are constant. The sign of n-type elements coefficient is negative while the sign of p-type element coefficients is positive for the Seebeck coefficients values. Then, for materials 1 and 2, we have next equations

$$\alpha_1 = [0.2068\ T + 138.78] \times 10^{-6} \quad \text{and} \quad \alpha_2 = \left[-62675 + 1610\ T - 2.3\ T^2\right] \times 10^{-6} \quad (51)$$

5.4. Special case: single-stage TEMC performance analysis

In this section, we analyse a single-stage system to compare with two-stage system to show the differences between both systems. Thereby, we calculate the two important parameters: COP and Q_c versus electric current; and COP and Q_c versus geometric parameter (w), for both materials. CPM models are compared with TDPM model, for this purpose, in all figures are shown results obtained considering Thomson effect (solid lines) and results using the ideal equation (dashed lines). **Figure 7** shows the COP_1, $Q_{c,1}$ and COP_2, $Q_{c,2}$ for materials, M_1 and M_2 respectively, as a function of the electric current. The maximum values of COP and Q_c are reached when the Thomson effect is considered, better cooling power is obtained with lower values of β. Results show that material M_1 achieves higher values of cooling power Q_c and COP than material M_2. The COP for material M_1 is 15.1% more than for material M_2 and Q_c for material M_1 is 40.12% more than for materialM_2.

Now, according to optimal electric current values, determined in the previous section, we show the effect of the semiconductor geometric parameters on the $COP(w)$ and $Qc(w)$ of the system. **Figure 8** shows that, for COP and Q_c, material M_1 has better results in both cases than material M_2. The COP of material M_1 is 21.18% higher than that for material M_2 and the Q_c value in material M_1 is 14.85% higher than for materialM_2.

5.5. Hybrid two-stage TEMC system

Now, we analyse a hybrid two-stage TEMC, that is, a system with a different thermoelectric material in each stage. Homogeneous system can also be analysed, this can be achieved by placing the same materials in both stages, as is shown in [27]. We focus on analysing two-stage hybrid systems, where two temperature gradients are generated and, therefore we must
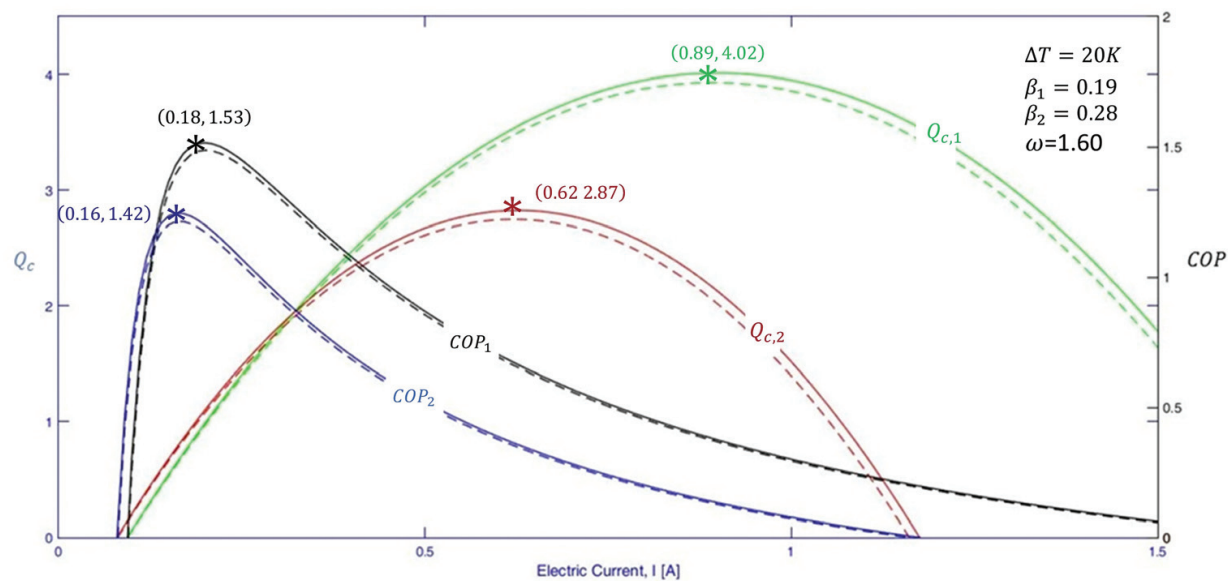
Figure 7. Single-stage coefficient of performance, $COP(I)$, and cooling power, $Q_c(I)$, for both materials M_1 and M_2. Solid lines calculated with Thomson effect and dashed lines considering ideal equation.
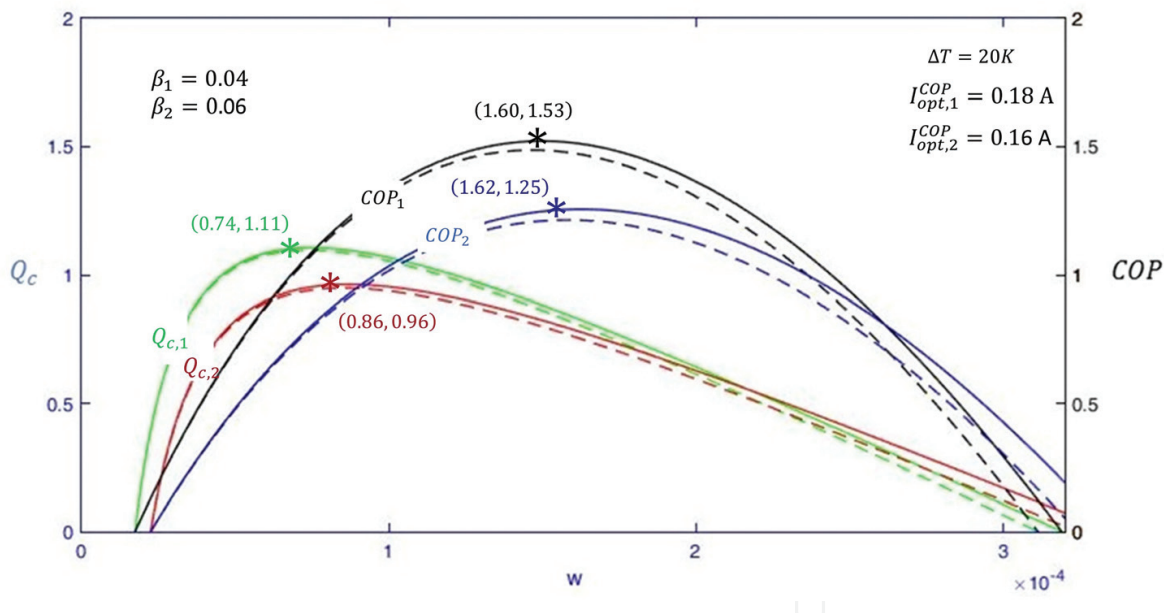
Figure 8. Single-stage $COP(w)$ and $Q_c(\omega)$ for both materials, using optimal electric currents I_{opt}^{cop}. Solid lines calculated with Thomson effect and dashed lines considering ideal equation.

analyse which material works better in each stage. Thus, we determine the optimum thermo-electric material arrangement for the best performance of the TEMC system. For this purpose, two configurations of materials in the hybrid two-stage TEMC model are considered: (a) materials M_1 and M_2 are used in the first and the second stage, respectively; and the inverse system (b) materials M_2 and M_1 are used in the first and the second stage, respectively.

5.5.1. Average system temperature, T_m

A two-stage TEMC consists of n_1 and n_2 thermocouples in the first and second stages, respectively. The heat flux at the cold side, Q_{c1}, and the heat flux at the hot side, Q_{h1}, in the first stage, and for the second stage, Q_{c2} and Q_{h2}, respectively. Thus, heat flux equations in the first stage are [31],

$$Q_{c1} = n_1\left[\alpha_1 I T_{c1} - K_1(T_m - T_{c1}) - 1/2R_1I^2 + \tau_1 I(T_m - T_{c1})\right] \tag{52}$$

$$Q_{h1} = n_1\left[\alpha_1 I T_m - K_1(T_m - T_{c1}) + 1/2R_1I^2 - \tau_1 I(T_m - T_{c1})\right] \tag{53}$$

and for the second stage,

$$Q_{c2} = n_2\left[\alpha_2 I T_m - K_2(T_{h2} - T_m) - 1/2R_2I^2 + \tau_2 I(T_{h2} - T_m)\right] \tag{54}$$

$$Q_{h2} = n_2\left[\alpha_2 I T_{h2} - K_2(T_{h2} - T_m) + 1/2R_2I^2 - \tau_2 I(T_{h2} - T_m)\right] \tag{55}$$

For a hybrid system (different materials in each stage), from equations (53) and (54), we obtain the temperature between stages, Tm,

$$T_m = \frac{-\frac{1}{2}I^2(R_1n_1 + R_2n_2) + \frac{1}{2}I(\tau_2 n_1 T_{h2} - \tau_1 n_1 T_{c1}) - K_2 T_{h2}n_1 - K_1 T_{c1}n_1)}{In_1\left(\alpha_1 - \frac{1}{2}\tau_1\right) + In_2\left(\frac{1}{2}\tau_2 - \alpha_2\right) - K_1n_1 - K_2n_2} \tag{56}$$

### 5.5.2. Dimensionless temperature distribution

For the hybrid two-stage TEMC system, the best configuration of semiconductor thermoelectric materials and its optimal geometric parameters is found in this section. For calculations we use a cross-sectional area of $A_c = 4.9 \times 10^{-9}m^2$ and element length of $L = 15\mu m$, with a total number of thermocouples of $n_1 = n_2 = 100$ in the first and second stages, respectively. **Figure 9** shows the dimensionless spatial temperature distributions, for cases (a) and (b) mentioned earlier. An important factor to analyse in the graphic is the maximum values of the temperature distribution in each stage. When the value of the derivative is to be $d\theta/d\xi > 0$, the semiconductor material is able to absorb a certain amount of heat, that is, Thomson heat acts by absorbing heat. For the case when the value of the derivative is to be $d\theta/d\xi < 0$, a release of heat occurs in the semiconductor, that is, Thomson heat acts by liberating heat. From **Figure 9**, maximum temperature distribution values in stage 1, $\theta = 1.06$, is near to the junction with stage 2, which is desirable because in the first stage, the system must absorb higher amount of heat to later be released in stage 2. Thereby, dimensionless temperature distribution, θ, as a function of the length, ξ, shows that a lower temperature distribution is required in the first stage and that higher values of temperature distribution are required in the second stage; this is achieved by choosing the optimal arrangement of materials between the two stages. According to this last statement, case (a) is the best configuration of materials to improve the TEMC.

5.5.3. Analysis and coefficient of performance and cooling power (Q_c)

Figure 10 shows COP and Q_c for the TEMC system for cases (a) and (b) described previously. Case (a) reaches best cooling power and coefficient of performance values. Notice that the
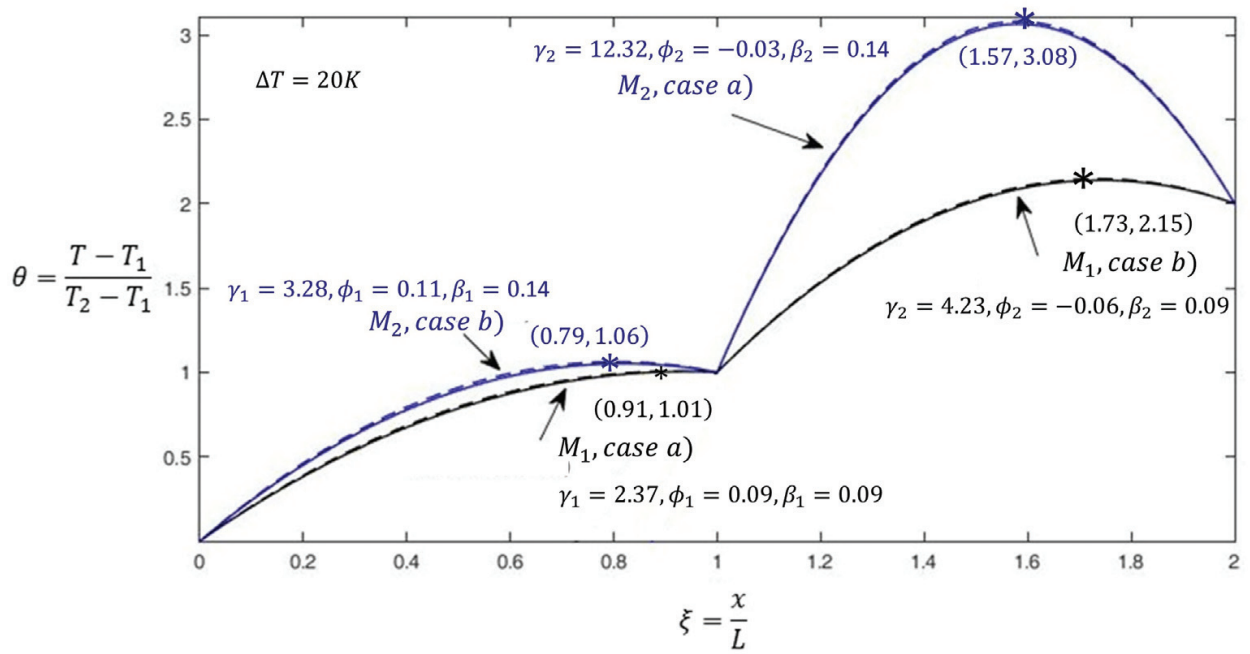
Figure 9. Hybrid two-stage TEMC. Dimensionless temperature distribution, $\theta(\xi)$. Case (a): material M_1 is placed in stage 1 (black line) and material M_2 in stage 2 (blue line). Case (b): material M_2 is placed in stage 1 (blue line) and material M_1 in stage 2 (black line). Solid lines calculated with Thomson effect and dashed lines considering ideal equation.
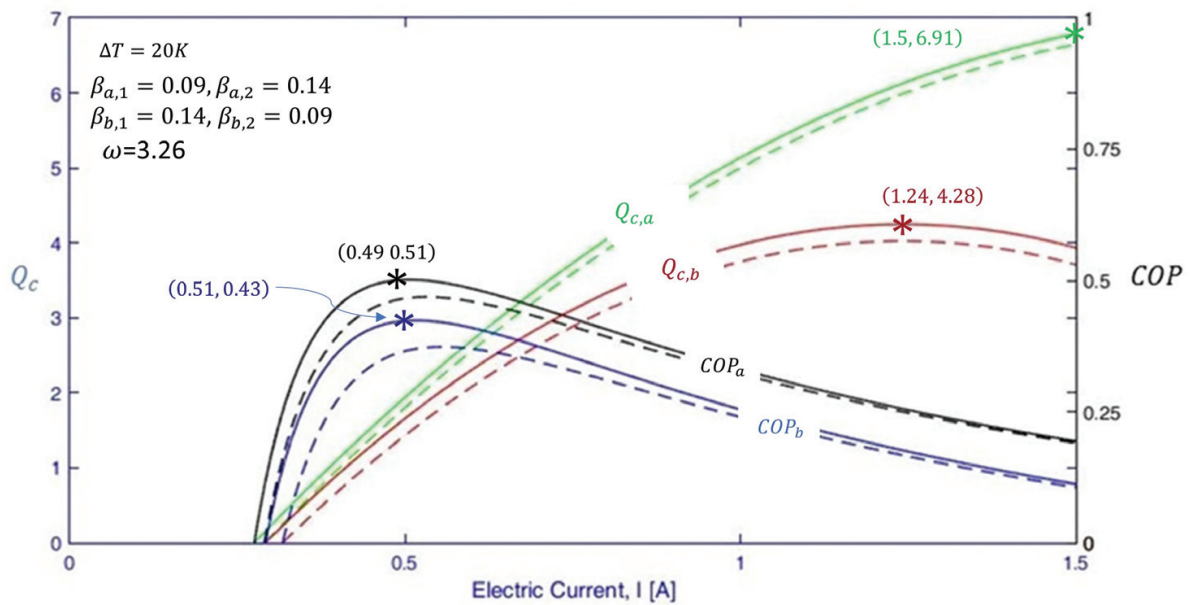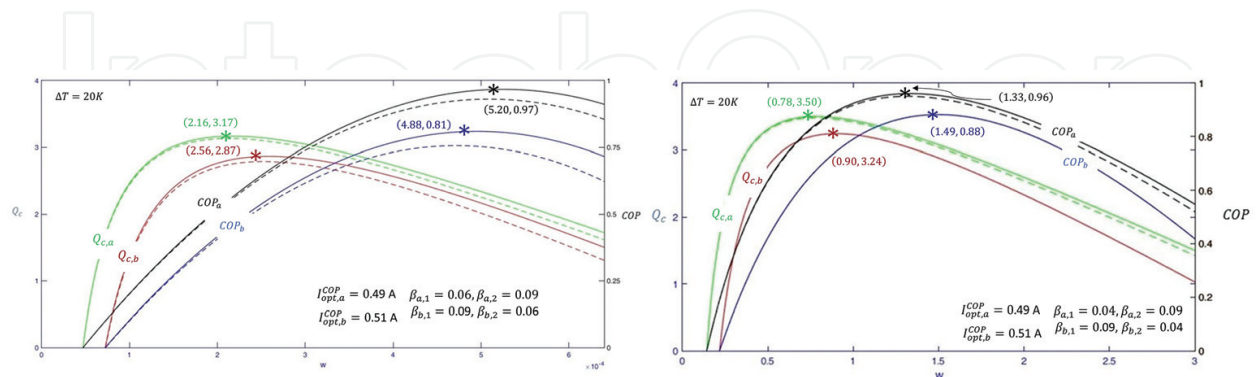

Figure 10. Hybrid two-stage TEMC. $COP(I)$ and $Q_c(I)$ for cases (a) and (b) with $w = w1 = w2$. Solid lines calculated with Thomson effect and dashed lines considering ideal equation.

$COP^{\beta}_{\max}(a)$ is 19.05% better than $COP^{\beta}_{\max}(b)$. It is clear from the graphic that for the same current values, cooling power values for the case (a) are always over those of the case (b).

5.5.4. Optimization analysis according to the geometric parameter W

In this section, we analyse the physical sizes, length and the cross-sectional area of the thermocouples, when the two stages are related each other. We present an optimization procedure of a two-stage TEMC system, on COP and Q_c, by introducing a geometric parameter, $W = \omega_1/\omega_2$. The effect of the parameter W on COP and Q_c is analysed when (1) $\omega_1 = \omega_2$ and (2) when $\omega_1 \neq \omega_2$. **Figure 11** (a) shows best optimal material configuration for $COP(w)$ and Q_c (w), which turns out to be case (a) where material M_1 is placed in the first stage and material M_2 in the second stage. Results proved that, higher area-length ratio values do not improve Q_c, on the contrary, the cooling power improves for lower values of w. COP and Q_c increases by 19 and 10.5%, respectively, from case (a) to case (b). The most relevant case, geometric parameters $\omega_1 \neq \omega_2$, is analysed. In this case, we set $\omega_2 = 3.26 \times 10^{-4}$ m to be a constant value. **Figure 11** (b) shows $COP(W)$ and $Q_c(\omega)$ where it is noted that COP increases by 8.9% and Q_c increases 6.27% in case (a) compared with case (b). From this last result, it is important to note that although the performance of TEC systems is affected by combination of different materials, it is also affected by the material configuration and the system geometry as well. These results offer a novel alternative in the improvement of thermoelectric systems, when they are used as coolers. Results shown in this chapter are based only on theory of thermoelectricity to optimize a TEMC system, according to geometric parameters. However, parameters as length and cross-sectional area of the semiconductor elements are based on studies which validated similar results with experimental data [32, 33]. In micro-refrigeration, an important problem is the fact of handle heat flux in a small space and it has been proved that thermal interface resistance has beneficial or detrimental effects on cooling performance [34]. For calculation, contact resistances between stages are not considered, since it is known that thermal resistances exist in the interfaces, which are large when the cross-sectional areas are very dissimilar in the stages and negligible for similar cross-sectional areas [35, 36]. Present work can be useful as theoretical

Figure 11. Hybrid two-stage TEMC. (a) $COP(\omega)$ and $Q_c(\omega)$ when $\omega_1 = \omega_2$. (b) $COP(W)$ and $Q_c(\omega)$ when $\omega_1 \neq \omega_2$. Solid lines calculated with Thomson effect and dashed lines considering ideal equation.

basis for future research in the experimental area, development and design of thermoelectric multistage coolers.

6. Conclusions

In this chapter, Thomson effect and leg geometry parameters on performance in a hybrid two-stage TEC were evaluated. For this purpose, the basics of two-stage thermoelectric cooler devices are analysed according to one dimension out-of-equilibrium thermodynamics using TDPM model. Two different semiconductor materials were used in all calculations. Results show, Thomson effect leads to a slight improvement on the performance and when the ratio of Thomson coefficients between both stages, $\tau_r = \tau_1/\tau_2$, increases, more cooling power can be achieved. We show that it is convenient to analyse optimal configuration of materials that must be used in each stage, showing that the material with a higher value of Seebeck coefficient must be place in the first stage. The main interest is to improve cooling power, thereby, a new procedure based on optimum leg geometric parameters of the semiconductor elements, is presented. Our analysis shows that, hybrid system reaches maximum cooling power, 15.9% greater than the one-stage system, for the case when the geometric parameter is $\omega_1 \neq \omega_2$. An important advantage of this work is that result can be confirmed in laboratories, as prototypes are made by mainly using bismuth telluride, which is the basis of the materials we use in all calculations.

Acknowledgements

Conflict of interest

The authors declare no conflict of interest.

Author details

Pablo Eduardo Ruiz-Ortega[1], Miguel Angel Olivares-Robles[1]* and Amado F. Garcia Ruiz[2]

*Address all correspondence to: molivares67@gmail.com

1 SEPI-Esime Culhuacan, Instituto Politecnico Nacional, Ciudad de Mexico, Mexico

2 UPIICSA, Instituto Politécnico Nacional, Ciudad de Mexico, Mexico

References

[1] Julian G, Robert H, Osgood R, Jurgen P, Hans W, editors. Introduction to Thermoelectricity. Springer Berlin: Springer Series in Material Science; 2010. 249 p. DOI: 10.1007/978-3-642-00716-3

[2] Ioffe A. Semiconductor Thermoelements and Thermoelectric cooling. London: Infosearch Limited; 1957. 185 p

[3] Goupil C, Seifert W, Zabrocki K, Muller E, Snyder G. Thermodynamics of thermoelectric phenomena and applications. Entropy. 2011;**13**:1481-1517

[4] Burshteyn A. Semiconductor Thermoelectric Devices. London: Temple Press; 1964

[5] El-Genk M, Saber H, Caillat T. Efficient segmented thermoelectric unicouples for space power applications. Energy Conversion and Management. 2003;**44**:1755-1772

[6] Di L, Fu-Yun Z, Hong-Xing Y, Guang-Fa T. Thermoelectric mini cooler coupled with micro thermosiphon for CPU cooling system. Energy. 2015:1-8

[7] Diana E, Elena O. A review on thermoelectric cooling parameters and performance. Renewable and Sustainable Energy Reviews. 2014;**38**:903-916

[8] Yang R, Chen G, Snyder G, Fleurial J. Multistage thermoelectric microcoolers. Journal of Applied Physics. 2004;**95**:8226-8232

[9] Cheng Y, Shih C. Optimizing the arrangement of two-stage thermoelectric coolers through a genetic algorithm. JSME International Journal. 2006;**49**:831-838

[10] Yang C, Di L, Fu-Yun Z, Jian-Feng T. Performance analysis and assessment of thermoelectric micro cooler for electronic devices. Energy Conversion and Management. 2016;**124**:203-211

[11] Meng F, Chen L, Sun F. Effects of temperature dependence of thermoelectric properties on the power and efficiency of a multielement thermoelectric generator. Energy & Environment. 2012;**3**:137-150

[12] Huang M, Yen R, Wang A. The influence of the Thomson effect on the performance of a thermoelectric cooler. International Journal of Heat and Mass Transfer. 2005;**48**:413-418

[13] Fabián M, Gao M, Alvarez Q. Enhanced performance thermoelectric module having asymmetrical legs. Energy Conversion and Management. 2017;**148**:1372-1381

[14] Callen H. The application of Onsager's reciprocal relations to thermoelectric, thermomagnetic, and galvanomagnetic effects. Physics Review. 1948;**73**:1349-1358

[15] Zemansky M. Heat and Thermodynamics. 5th ed. New York: McGraw-Hill; 1968

[16] Onsager L. Reciprocal relations in irreversible processes. II. Physics Review. 1931;**38**:2265-2279. DOI: 10.1103/PhysRev.38.2265

[17] Seifert W, Ueltzen M, Müller E. One-dimensional modelling of thermoelectric cooling. Physica Status Solidi. 2002;**194**:277-290

[18] Zabrocki K, Müller E, Seifert W. One-dimensional modeling of thermogenerator elements with linear material profiles. Journal of Electronic Materials. 2010;**39**:1724-1729

[19] Rowe DM. CRC Handbook of Thermoelectics. Boca Raton: CRC Press; 1995. pp. 214-219

[20] Min G, Rowe DM. Improved model for calculating the coefficient of performance of a Peltier module. Energy Conversion and Management. 2000;**2**(41):163-171

[21] Lee H. The Thomson effect and the ideal equation on thermoelectric coolers. Energy. 2013;**56**:61-69

[22] Xuan X. Analyses of the performance and polar characteristics of two-stage thermoelectric coolers. Semiconductor Science and Technology. 2002;**17**:414-420

[23] Chen J, Zhou Y, Wang H, Wang J. Comparison of the optimal performance of single- and two-stage thermoelectric refrigeration systems. Applied Energy. 2002;**73**:285-298

[24] Liu J, Wen C. Examination of the cooling performance of a two-stage thermoelectric cooler considering the Thomson effect. Numerical Heat Transfer. 2011;**60**:519-542

[25] Chen J, Yan Z, Wu L. Non-equilibrium thermodynamic analysis of a thermoelectric device. Energy. 1997;**22**:979-985

[26] Goupil C. Continuum Theory and Modeling of Thermoelectric Elements. Berlin: Wiley-VCH; 2016. 353 p. ISBN: 978-3-527-41337-9

[27] Ruiz E, Olivares MA. Analysis of a hybrid thermoelectric microcooler: Thomson heat and geometric optimization. Entropy. 2017;**19**:312. DOI: 10.3390/e19070312

[28] Ruiz E, Olivares MA. Analisis del Calor de Thomson en un Sistema Termoelectrico Unidimensional de dos Etapas. In: Semana Nacional de Ingenieria Electronica. Vol. 108. Celaya Mexico: Pistas Educativas; 2014. pp. 576-593

[29] Matthew M, Kenechi A, Parthib R, Corey E, Reddy B, Minking K. Geometric optimization of thermoelectric elements for maximum efficiency and power output. Energy. 2016;**112**:388-407

[30] Sahin A, Yilbas B. The thermoelement as thermoelectric power generator: effect of leg geometry on the efficiency and power generation. Energy Conversion and Management. 2013;**65**:26-32

[31] Karimi G, Culham J, Kazerouni V. Performance analysis of multi-stage thermoelectric coolers. International Journal of Refrigeration. 2011;**34**:2129-2135

[32] Snyder GJ, Fleurial J-P, Caillat T, Yang RG, Chen G. Supercooling of Peltier cooler using a current pulse. Journal of Applied Physics. 2002;**92**:1564

[33] Yang R, Chen G, Kumar AR, Snyder GJ, Fleurial JP. Transient cooling of thermoelectric coolers and its applications for microdevices. Energy Conversion and Management. 2005;**46**:1407-1421

[34] Ju YS, Ghoshal U. Study of interfac eeffects in thermoelectric microrefrigerators. Journal of Applied Physics. 2000;**88**(7):4135-4139

[35] Yazawa K, Ziabari A, Kho Y, Shakouri A. Cooling power optimization for hybrid solid-state and liquid cooling in integrated circuit chips with hotspots. IEEE ITHERM Conference; 2012. pp. 99-106

[36] Kho Y, Yazawa K, Shakouri A. Performance and mass optimization of thermoelectric microcoolers. International Journal of Thermal Sciences. 2015;**97**:143-151